IBRACON Structures and Materials Journal
Revista IBRACON de Estruturas e Materiais
ISSN 1983-4195 ismj.org

ORIGINAL ARTICLE

Sonicating polycarboxylate-based superplasticizer for application in cementitious matrix

Sonicação de superplastificante à base de policarboxilato para aplicação em matrizes cimentícias

Laura Silvestro[a,b]
Artur Spat Ruviaro[a]
Geannina Terezinha dos Santos Lima[a]
Paulo Ricardo de Matos[c]
Erich Rodríguez[d]
Philippe Jean Paul Gleize[a]

[a]Universidade Federal de Santa Catarina, Department of Civil Engineering, Florianópolis, SC, Brasil
[b]Universidade Federal Tecnológica do Paraná, Guarapuava, PR, Brasil.
[c]Universidade Federal de Santa Maria, Coordenadoria Acadêmica, Campus Cachoeira do Sul, Cachoeira do Sul, RS, Brasil
[d]Universidade Federal de Santa Maria, Department of Structures and Civil Construction, Santa Maria, RS, Brasil

Received 15 April 2022
Accepted 11 August 2022

Abstract: Sonication is widely used for nanomaterials dispersion in cementitious matrices. Polycarboxylate-based superplasticizer (SP) admixtures are usually incorporated in the aqueous nanomaterials suspension before sonication to improve the dispersion of these materials. Nevertheless, the effect of sonicating SP on its molecular structure or dispersing performance has not been fully investigated. This work assessed the effect of sonicating a commercial SP at 20 kHz, 750 W power, 50 or 80% amplitude, during 15 and 30 min. Initially, the sonication effect was evaluated in aqueous suspension by determining the SP size distribution (through dynamic light scattering – DLS) and zeta potential. Subsequently, the aqueous SP suspensions were used for Portland cement paste production. Rheological tests up to 120 minutes and compressive strength at 14 and 28 days were conducted. DLS and zeta potential results suggested that sonication reduce the size of SP chains. As a result, SP sonication increased the initial dynamic yield stress, viscosity, and hysteresis area of cement pastes. In contrast, SP sonication improved its time-dependent dispersing performance, resulting in pastes with reduced viscosity from 80 minutes onwards. Finally, SP sonication did not affect the compressive strength of cement pastes at 14 and 28 days of hydration. Overall, when SP is sonicated together with nanoparticles for application in cementitious matrices, the effect of sonicating the chemical admixture must be considered when the fresh-state properties of the composite are evaluated.

Keywords: superplasticizer, sonication, cement paste, rheology.

Resumo: A sonicação é amplamente utilizada para dispersão de nanomateriais em matrizes cimentícias. Aditivos superplastificantes à base de policarboxilato (SP) são geralmente incorporados na suspensão aquosa de nanomateriais antes da sonicação para melhorar a dispersão desses materiais. No entanto, o efeito da sonicação na estrutura molecular e no desempenho de dispersão do SP não foi totalmente investigado. Este trabalho avaliou o efeito da sonicação de um SP comercial a 20 kHz, potência de 750 W, amplitude de 50 e 80%, durante 15 e 30 min. Inicialmente, o efeito de sonicação foi avaliado em suspensão aquosa, determinando a distribuição de tamanho do SP (através de espalhamento dinâmico de luz – DLS) e potencial zeta. Posteriormente, as suspensões aquosas de SP foram utilizadas para a produção de pastas de cimento Portland. Foram realizados ensaios reológicos durante os primeiros 120 minutos de hidratação e a resistência à compressão foi avaliada aos 14 e 28 dias. Os resultados do potencial zeta e DLS sugeriram que a sonicação reduz o tamanho das cadeias de SP. Como resultado, a sonicação do SP aumentou a tensão de escoamento dinâmica inicial, a viscosidade e a área de histerese das pastas de cimento. Em contraste, a sonicação SP melhorou seu desempenho de dispersão ao longo do tempo, resultando em pastas com viscosidade reduzida a partir de 80 minutos. Finalmente, a sonicação SP não afetou a resistência à compressão das pastas de cimento aos 14 e 28 dias de hidratação. Em geral,

Corresponding author: Laura Silvestro. E-mail: laurasilvestro1@gmail.com
Financial support: CAPES, CNPq, FAPESC from Brazil provided financial support for the study.
Conflict of interest: Nothing to declare.
Data Availability: The data that support the findings of this study are available from the corresponding author, LS, upon reasonable request.

quando o SP é disperso via sonicação juntamente com nanopartículas para aplicação em matrizes cimentícias, o efeito de sonicação do aditivo químico deve ser levado em consideração quando as propriedades de estado fresco do compósito são avaliadas.

Palavras-chave: superplastificante, sonicação, pastas de cimento, reologia.

How to cite: L. Silvestro, A. S. Ruviaro, G. T. S. Lima, P. R. Matos, E. Rodríguez, and P. J. P. Gleize, "Sonicating polycarboxylate-based superplasticizer for application in cementitious matrix" *Rev. IBRACON Estrut. Mater.*, vol. 16, no. 2, e16205, 2023, https://doi.org/10.1590/S1983-41952023000200005

1 INTRODUCTION

Sonication is widely used for nanomaterials dispersion for application in cementitious matrices, such as carbon nanotubes [1]–[5], nanosilica [6]–[10], silicon carbide nanowhiskers [11]–[13], nano-clay [14], [15], silica fume [16], among others. The high performance of nanoparticles used in cementitious materials is mainly due to their high specific surface area, which – in most cases – is reduced by its susceptibility to agglomeration. This effect reduces the mechanical strength of these cementitious nanocomposites. Thus, sonication is commonly used for enhancing the nanomaterials' dispersion. In this dispersion process, a cavitation field produces microbubbles that promote the nanomaterial agglomerates exfoliation [17], as well as (in some cases) the sonication promotes the formation of charged holes (h^+) on the nanoparticles' surface [18]. The nanomaterials' dispersion degree via sonication is a function of several aspects such as duration, intensity, output frequency, energy applied, sonicator type (bath or tip) and transducer oscillator, temperature, content, as well as characteristics of the nanomaterial dispersed [19], [20]. Tip sonicators provide denser energy compared to bath sonicators, where the ultrasounds are irradiated from the edge of the metallic tip to a smaller area around it. This concentrates the cavitational activity area, and a stronger spray is formed, which also produces an aggressive agitation of the solution [17]. Thus, the dispersion through tip sonicators usually requires a shorter duration than bath sonicators [20].

According to the literature, most of the studies with carbon nanotube addition in cement-based materials used sonication treatment to improve the nanomaterial dispersion, combined with the incorporation of dispersants (e.g., polycarboxylate-based superplasticizers – SP) [21]. The use of SP for nanomaterial's dispersion is attractive due to the compatibility of these admixtures with cement particles. Furthermore, this approach avoids using other types of dispersants (e.g., surfactants), reducing the possibility of incompatibility between matrix components and cement particles [22]. In this context, Sindu and Sasmal [23] reported that the use of surfactants like Sodium dodecyl benzene sulphonate (SDB), sodium lauryl sulphate (SLSD), and Triton X-100 (TX) for CNTs dispersion generally reduced the 28-day compressive and tensile strengths of cementitious composites compared to plain cement paste. This behavior was attributed to the surfactants that may have hindered the Portland cement hydration and increased the content of air trapped into the matrix, as evidenced by the density of the composites [23].

Concerning the duration of the sonication process for nanomaterials dispersion, long periods are usually used. For instance, Ma et al. [24] dispersed CNTs in mixing water with a polycarboxylate-based SP through sonication in a high-intensity sonicator (500 W) for 1 hour at 40% amplitude. Mohsen et al. [25] sonicated an aqueous CNTs suspensions with polycarboxylate-based SP for 30 minutes at 20% amplitude. Similarly, Sedaghatdoost and Behfarnia [26] dispersed CNTs and polycarboxylate-based SP by sonication for 30 minutes. According to Assi et al. [20], CNTs' dispersion via sonication is usually conducted during a period from 20 to 45 minutes. In this context, the SP usually is added to aqueous suspensions of nanomaterials before the sonication process, i.e., it is dispersed together with the nanomaterial. Several studies have reported that excessive sonication energy can damage the CNTs and, therefore, compromise the ability to enhance the mechanical properties of composites with the incorporation of these nanomaterials [27]–[29]. However, the effect of the sonication process on the molecules of SP admixtures used in cementitious composites has not yet been reported.

In other research fields, previous studies have reported that sonication is used for the degradation of surfactants. For instance, Dehghani et al. [30] used an ultrasonic bath to evaluate the degradation of an anionic surfactant. The results reported by the authors indicated that the duration of sonication plays an important role in the integrity of the surfactant. The surfactant degradation rate gradually increases with the process duration. In turn, an opposite trend was observed regarding the surfactant concentration: there was a decrease in the surfactant degradation rate with the increase of its concentration. Campbell and Hoffmann [31] also assessed surfactants degradation via sonication. The results showed that the degradation rate increased with the increase in power density applied. Similarly, Bhandari et al. [32] investigated the use of ultrasonic for degradation of sodium dodecyl sulfate surfactant in order to reduce water resources contamination.

Considering that sonication can cause the degradation of surfactants, it is expected to influence admixtures developed for application in cementitious matrices. Nevertheless, the effect of sonication on admixtures for cement-based materials has not been fully investigated. One of the only works on this topic is from Poinot et al. [33]. The authors observed that sonication of commercial water retention admixtures (hydroxypropyl methyl cellulose and hydroxypropyl guar) promoted an expressive molecular weight reduction of the molecules evaluated.

Although sonication is widely used for the dispersion of nanomaterials aiming for application in cementitious matrices, the effect of this dispersion process on the polycarboxylate-based superplasticizer admixtures has not been fully assessed. Thus, this work aimed to evaluate the effect of this dispersion process on the size distribution and zeta potential when a commercial polycarboxylate SP was sonicated. Furthermore, the effect of sonication of SP admixture on the rheology and compressive strength of Portland cement pastes was also evaluated.

2 MATERIALS AND METHODS

2.1 Materials

Portland cement (PC) was used for paste production. Table 1 details its chemical composition determined by X-ray fluorescence (XRF) using an EDX-7000 (Shimadzu, Tokyo, Japan) equipment, in addition to its physical properties. The size distribution of PC was evaluated through laser diffraction in air dispersion using a Particle Size Analyzer S3500 (Microtrac, Pennsylvania, USA) equipment. The specific surface area (SSA) of the PC was determined through the Brunauer–Emmett–Teller (BET) method (Autosorb Quantachrome Instruments, Florida, USA) with nitrogen adsorption. The sample was pre-heated at 40 ^{0}C during 12 h. The mineralogical composition of PC presented in Table 2 was obtained by X-ray diffraction (XRD) and Rietveld analysis. The analysis was conducted using an X'Pert Pro (PANalytical, Almelo, The Netherlands) diffractometer operating at 45 kV and 40 mA with CuK$\alpha_{1,2}$ radiation (λ = 1.5418 Å), scanning range of 7–70^{0} 2θ, and step size of 0.0167° 2θ. Rietveld quantitative phase analysis (QPA) was conducted using TOPAS v5 (Bruker) software and ICSD database (also detailed in Table 2).

Table 1. Chemical composition determined by XRF and physical properties of the cement used.

Property	Value
Al_2O_3 (wt.%)	4.40
SiO_2 (wt.%)	18.62
Fe_2O_3 (wt.%)	3.00
CaO (wt.%)	62.75
MgO (wt.%)	3.80
SO_3 (wt.%)	3.08
Loss on ignition at 950 ^{0}C (wt.%)	3.41
Insoluble residue	0.94
D_{10} (µm)	2.91
D_{50} (µm)	11.1
D_{90} (µm)	29.1
Mean diameter (µm)	13.1
Density (kg/m^3)	3,100
BET specific surface area (m^2/g)	2.22

Table 2. Mineralogical composition of the cement used obtained by XRD-Rietveld QPA.

Phase	ICSD code	PC (wt. %)
C_3S M1	*	44.11
C_3S M3	94742	17.36
C_2S á	81097	0.75
C_2S â	79550	10.33
C_3A cub	1841	2.70
C_4AF	9197	8.02
Goergeyite	30790	2.57
Syngenite	157072	2.42
Periclase	9863	1.12
Bassanite	69060	0.81
Gypsum	151692	3.43
Calcite	73446	5.93
Quartz	174	0.45
R_{wp} (%)		5.11

* Not in ICSD; crystal structure from Noirfontaine et al. [34].

A commercial polycarboxylate-based superplasticizer (SP) was evaluated in this study. The SP had a solid content of 42.0 wt.%, density of 1,120 kg/m^3, and pH of 6.15 at 23°C. For SP characterization, Fourier transform infrared spectroscopy (FTIR) was conducted in a liquid sample. The test was carried out in a Cary 600 Series FTIR Spectrometer using the following parameters: analysis range from 500 to 4000 cm^{-1}, resolution of 2 cm^{-1}, and 32 accumulations. Figure 1 shows the FTIR spectrum of the SP. The absorption peaks around 3300-3400 and 1639 cm^{-1} are attributed to O–H bond of water [35]. The absorption peaks at 2924 and 2875 cm^{-1} can be assigned to the stretching vibration of C–H bond from aliphatic groups [36]. The peaks at 1455, 1349, 1247, 1087, and 950 cm^{-1} belong to CH_2, CH_3, C–O, C–O–C, and C–C bonds, respectively [35], [37]. These peaks are characteristic of aliphatic, carbonyl, and ether groups present in SP [38].

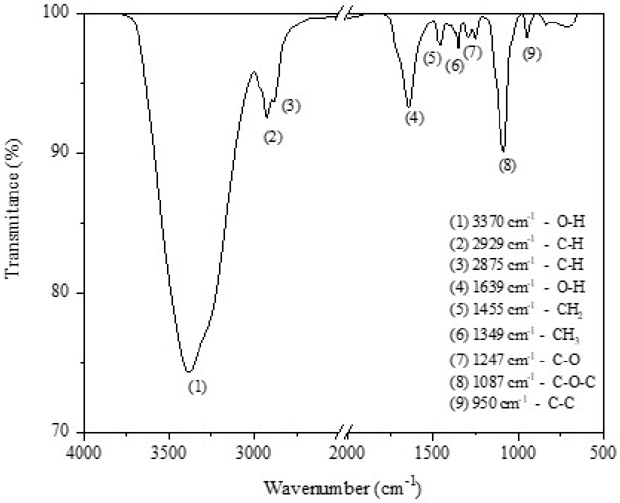

Figure 1. FTIR spectrum of the polycarboxylate-based SP.

2.2 Sample preparation

The SP aqueous dispersions evaluated are detailed in Table 3. The proportions of water and SP were defined to obtain cement pastes with a water-to-cement ratio of 0.4 and a SP content of 0.2 wt.% by weight of cement. Initially, fixed amounts of deionized water (48.0 g) and SP (0.24 g) were mixed and sonicated using a 13-mm ultrasonic probe VCX Serie Vibra-Cell, characterized by a maximum power of 750 W and frequency output of 20 kHz (Sonics & Materials Inc., Newtown, CT, USA). The solution was sonicated in a glass beaker of 50 ml, where the transductor probe was immersed at approximately 10 mm of the bottom, as illustrated in Figure 2. To prevent the samples from overheating, pulses of 20 seconds and resting of 20 seconds were alternated during the sonication process. Besides, the samples were sonicated in an ice bath for the same purpose. Two amplitudes (50 and 80%) and two duration times (15 and 30 minutes) of sonication were evaluated. Furthermore, a control sample (i.e., with superplasticizer not subjected to sonication) was also evaluated for comparison. After that, the SP aqueous dispersions were added to 120.0 g of cement and mixed for 2 minutes in a high-shear mixer at 10,000 rpm.

Table 3. SP aqueous dispersions evaluated.

Sample	Water (g)	SP (g)	Sonication parameters				
			Amplitude (%)	Duration (min)	Energy (J)	Energy (J/g of SP)	Temperature (^{0}C)
SP	48.00	0.24	-	-	-	-	-
SP-A50%-15 min	48.00	0.24	50	15	28,035.0	116,812.5	25
SP-A50%-30 min	48.00	0.24	50	30	56,146.0	233,941.7	25
SP-A80%-15 min	48.00	0.24	80	15	62,512.0	260,466.7	32
SP-A80%-30 min	48.00	0.24	80	30	125,537.0	523,070.8	32

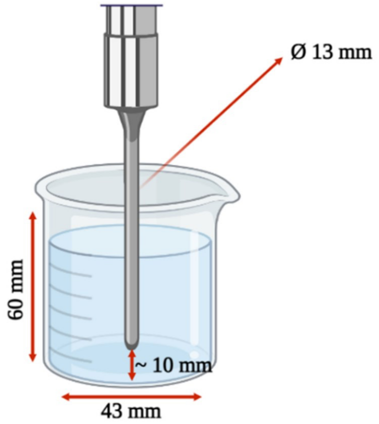

Figure 2. Schematic representation of the position of the ultrasonic probe in the glass beaker containing the aqueous SP solution.

2.3 Testing methods

2.3.1 Tests conducted in aqueous solution

For the SP aqueous solution characterization, zeta potential and size distribution measured by dynamic light scattering (DLS) were performed. The tests were carried out in a Zetasizer Nano (Malvern, UK). The analyses were conducted at 23 ^{0}C with a range from 3.8 nm to 100 µm. Before performing the analyses, the SP aqueous suspensions were vacuum filtered in a filter with a retention capacity of 7 µm to remove possible contaminants from the samples. A similar approach has been reported in previous studies [39]–[41].

2.3.2 Tests conducted in Portland cement pastes

Rheological tests were conducted in cement pastes using a Haake MARS III (Thermo Fisher Scientific, Waltham, MA, USA) rheometer at 23.0 °C. A hatched parallel-plate geometry with a diameter of 35.00 mm (Figure 3) and an axial gap of 1.000 mm were used. The test started 10 minutes after the contact of PC with water. Initially, a pre-shear at 100 s^{-1} was applied for 60 seconds to ensure the same analysis condition for all samples. Subsequently, the ascending flow curve was obtained by increasing the shear rate from 0.1 to 100 s^{-1} in 10 steps. Finally, the descending flow curve was determined by decreasing the shear rate from 100 to 0.1 s^{-1} in the same steps. In each step, the shear rate was kept for 10 seconds (previously defined as adequate for shear stress stabilization), and the last 3 seconds of each step were recorded. The data of the descending flow curve fitted using the Herschel-Bulkley (H-B) model, described in Equation 1. The equivalent plastic viscosity of cement pastes was calculated through Equation 2 [42]. The hysteresis area between the increasing and decreasing portions – associated with thixotropy – was also determined. The fluidity of the pastes was also elevated through the mini-slump test [43].

$$\tau = \tau_0 + K.\dot{\gamma}^n \tag{1}$$

$$\mu_{eq} = \frac{3K}{n+2} \cdot (\dot{\gamma}_{max})^{n-1} \tag{2}$$

where τ is the shear stress (Pa), τ_0 is the dynamic yield stress (Pa), $\dot{\gamma}$ is the shear rate (s^{-1}), K and n are respectively the consistency and the pseudoplastic parameters of the H-B model, and $\dot{\gamma}_{max}$ is the maximum shear rate applied.

To evaluate the variability of the rheological tests, two independent fresh pastes were tested for the following pastes: SP, SP-A80%-15 min, and SP-A80%-30 min. The mean values were adopted for the rheological parameters. The results exhibited good repeatability, where standard deviation values below 5.2% and 8.5% were observed respectively for the dynamic yield stress and the equivalent viscosity.

In addition, the samples SP, SP–A80%–15 min, and SP–A80%–30 min were selected for time-resolved rheological analyses to evaluate the influence of SP sonication condition on the rheology of pastes during the first 120 minutes hydration. These analyses were conducted with the same conditions previously described, performed each 10 min for 2 hours, resulting in 12 measurements over this time range. An insulation chamber was used to prevent mixing water evaporation (Figure 3).

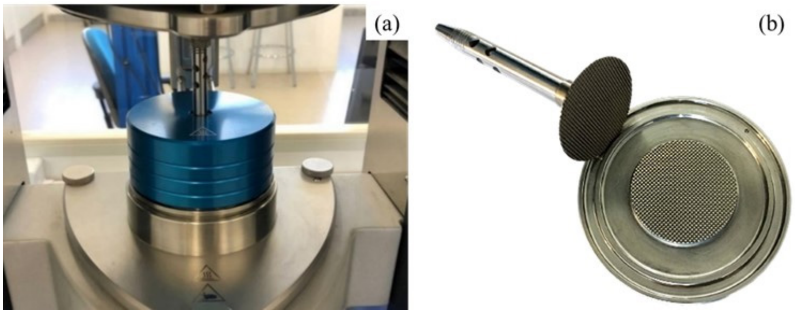

Figure 3. Rheological tests setup used. (a) Rheological tests setup with insulation chamber used to prevent the mixing water evaporation; (b) parallel-plate geometry with hatched surface.

Finally, the compressive strength of cement pastes was determined after 14 and 28 days of hydration. The test was performed following ASTM C1231 [44]. The mean compressive strength of each composition was calculated based on the results of 5 cylindric specimens with diameter of 20 mm and height of 26 mm. Analysis of Variance (ANOVA) was conducted on OriginPro software (OriginLab, Massachusetts, USA), considering a significance level of 0.05.

3 RESULTS AND DISCUSSIONS

3.1. Superplasticizer aqueous suspensions characterization

Figure 4 shows the size distribution of SP as received and after the sonication with an amplitude of 80% for 15 and 30 min. The results indicated that the SP had an average diameter of around 190 nm. Besides, the SP exhibited a polydispersity index (PDI) of 0.2, which indicated a monodisperse distribution [45]. The SP size diameter agrees with the hydrodynamic radius of a few tens of nanometers of usual polymers used in cement-based materials [39]. Note that this diameter is higher than those reported for polycarboxylate SP by some authors [40], [41]. Nevertheless, it should be considered that in the studies previously mentioned, the SP molecules were synthesized under controlled conditions. In contrast, the SP used in this research is a commercial organic admixture. Thus, the composition and all constituents of this admixture are not fully disclosed by the manufacturer due to confidentiality reasons. This may help to explain the higher average diameter of the SP used in this study compared to other reported in the literature. The DLS results showed that the sonication of SP promoted changes in the size distribution of the admixture. Overall, the sonication slightly shifted the size distribution to smaller values. Thus, SP aqueous dispersions sonication for 15 and 30 minutes increased the PDI by 170.0% (SP – A80% - 15 min) and 100.0% (SP – A80% - 30 min), respectively, compared to SP. These results indicated that sonication increased the heterogeneity of the SP aqueous dispersions. This suggests that sonication may reduce the length of SP chain, as further discussed in the rheological test results. This trend is in line with the results reported by Poinot et al. [33], where the authors observed reductions in the molecular weight of commercial water retention admixtures submitted to sonication.

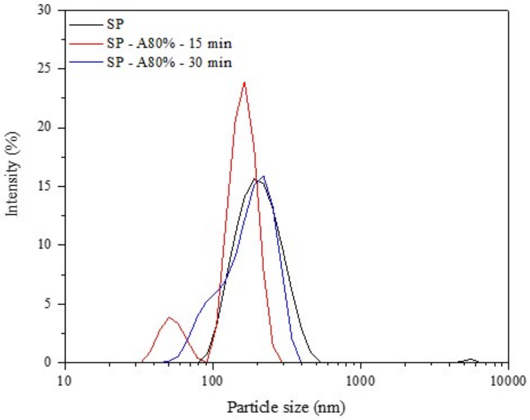

Figure 4. Size distribution of SP, SP - A80% - 15 min, and SP - A80% - 30 min aqueous dispersions, determined by DLS.

Figure 5 shows the zeta potential of SP, SP – A80% – 15 min, and SP – A80% – 30 min aqueous dispersions. All dispersions evaluated exhibited negative potential zeta values, which is attributed to the negative charge provided by the carboxylic groups (–COO–) present in the molecular structure of SP admixtures [46]. Furthermore, it was observed that increasing the sonication time increased the absolute value of zeta potential. This behavior may be related to the decrease in the chain length of SP with sonication (suggested by our size distribution results), which increases the amount of free carboxylic groups [47]. This trend is consistent with the previous studies that reported that SP molecules with shorter side chain lengths resulted in high absolute zeta potential values [48], [49]. Moreover, although these results indicated that sonication slightly improved the colloidal stability of SP, it should be noted that the particle dispersion (e.g., cement and/or nanomaterials) promoted by polycarboxylate SP comes mainly from steric hindrance [46], [50]. Feng et al. [51] reported that the side chain length possibly has a higher effect on the steric hindrance compared to the electrostatic repulsion of the functional groups. Thus, this increase in the absolute zeta potential values may not be associated with a greater dispersion capacity, as further discussed in the rheological test results.

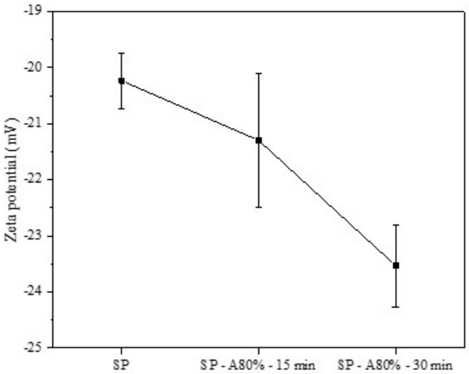

Figure 5. Zeta potential of SP, SP – A80% - 15 min, and SP – A80% - 30 min aqueous dispersions.

3.2. Paste rheological tests

Figure 6 exhibits the shear stress and viscosity curves of the cement pastes as a function of the shear rate, and Figure 7 summarizes the rheological test results. SP sonication slightly reduced the mini-slump values of the cement pastes compared to the reference sample with non-sonicated SP. Besides, it increased the dynamic yield stress, equivalent viscosity, and hysteresis area of cement pastes. For instance, increases of up to 13.4%, 16.7%, and 16.8% were observed for dynamic yield stress, viscosity, and hysteresis area, respectively, when SP was sonicated. However, no clear relationship between SP sonication amplitude and duration with the increase in the rheological properties was observed. Increasing the sonication time for a given amplitude apparently increased the viscosity and thixotropy (associated with the hysteresis area) of paste, but these differences may fall within the measurement error (see error bars in Figure 7). Besides, this trend did not occur for the yield stress and mini slump. This behavior is in line with the results reported by Malhotra [52]. The author also observed that in systems composed of hydroxypropyl cellulose and water, the cavitation intensity did not show a linear increase with the ultrasound intensity.

Overall, the rheological test results indicate that SP sonication reduced its dispersion capacity, supporting the hypothesis that sonication affected its molecular structure as suggested by our DLS and zeta potential results. According to Winnefeld et al. [47], the adsorption of polycarboxylate SP onto cement particles is affected by its molecular weight. Erzengin et al. [53] identified that the higher the density and length of side chains and the molecular weight of polycarboxylate SP, the higher the adsorption onto cement surface. In this context, Magarotto et al. [54] observed that the increase in molecular weight of polycarboxylate-based SP enhances the polymer adsorption and, therefore, the dispersing performance of the admixture. Peng et al. [55] also reported that polycarboxylate-based SP with a high molecular weight exhibited a more pronounced initial dispersing ability, resulting in lower yield stress than SP with a low molecular weight. A similar trend was identified in the study conducted by Palacios et al. [56]. The authors found that the polycarboxylate-based SP admixture with the highest molecular weight resulted in the lower yield stress value of slag-blended cement pastes, which was attributed to a higher steric repulsion effect. This trend is in line with previous studies regarding the adsorption of other types of polymers. Considering the adsorption equilibrium of polymers at interfaces, those with high molecular weight tend to preferentially adsorb [54]. By contrast, considering that sonication may have reduced the chain length of the SP molecules (see Section 3.1), it reduced the molecular weight for a given polymer concentration, reducing the particle dispersion ability.

Another aspect that should be stressed is that water sonication can produce hydrogen peroxide (H_2O_2) [57], [58]. Nevertheless, its effect on the fresh-state properties of cement pastes was not yet investigated. Thus, future studies should assess whether the formation of hydrogen peroxide occurs and how this can affect the rheological properties of cement-based materials.

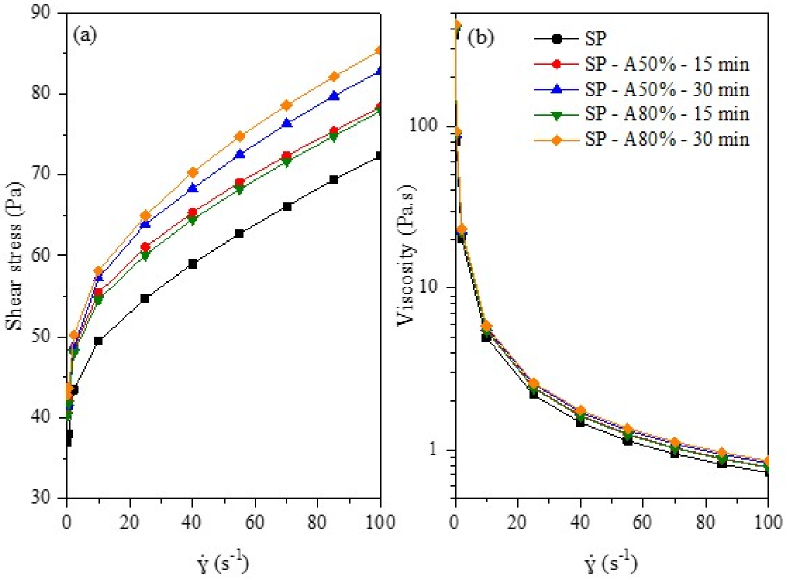

Figure 6. Flow curves (a) and viscosity vs. shear rate curves (b) of cement pastes evaluated after 10 min of hydration.

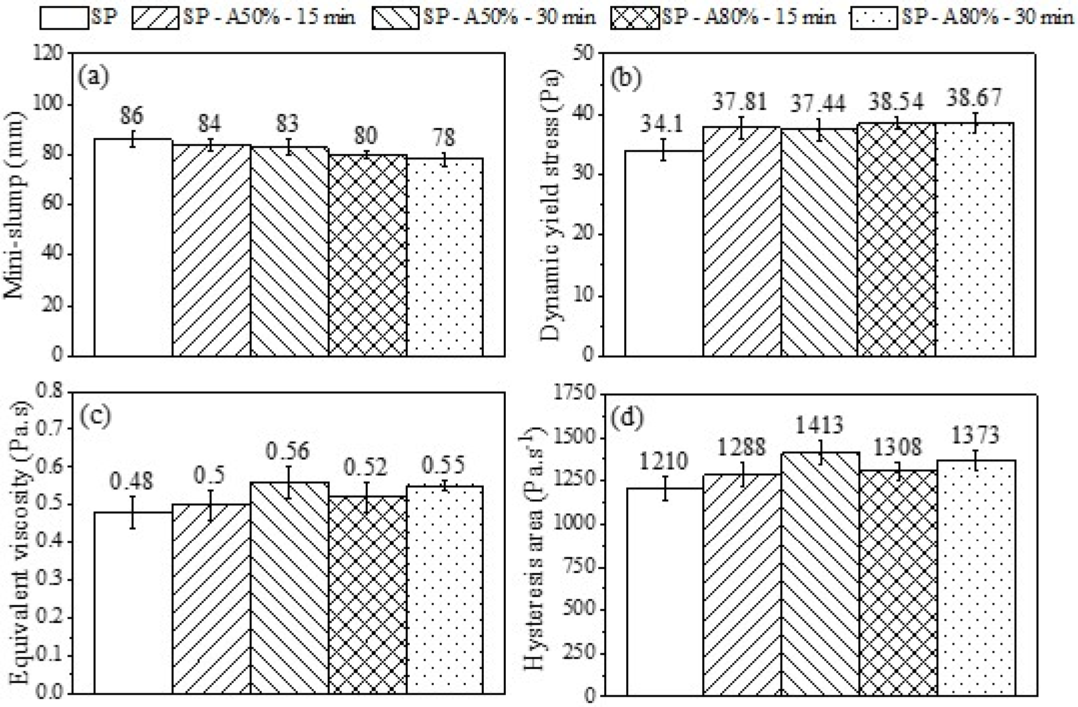

Figure 7. Fresh-state properties of the pastes at 10 minutes of hydration: mini-slump (a); dynamic yield stress (b); equivalent viscosity (c); and hysteresis area (d). Note: error bars in (a) correspond to ±1 standard deviation, while in (b)-(d) were estimated based on complementary tests.

Regarding the dispersing ability of SP over time, Figure 8 exemplifies the shear stress and viscosity curves as a function of the shear rate for the time-resolved tests. Figure 9 shows the dynamic yield stress and equivalent viscosity of SP, SP–A80%-15 min, and SP–A80%-30min pastes within the first 2 hours of hydration. As a general trend, the yield stress of the pastes was practically constant during the first 60 minutes of hydration, while a constant increase in viscosity was observed. However, from 60 minutes onwards, both yield stress and viscosity increased. A similar trend was observed in the study from Liu et al. [59], where the yield stress of a cement paste with polycarboxylate SP remained practically unchanged during the first 30 min, while between 30 and 180 min it showed a linear increase.

According to Rousel et al. [60], the yield stress of cement paste increases over time due to the combination of flocculation (already at a few seconds after stop shearing) and the progressive formation of C-S-H that form a rigid network. It is known that polycarboxylate-based SPs delay the hydration kinetics of Portland cement, either by Ca^{2+} ions complexation [61], the change in the morphology of hydrated phases [62], [63], or the hindered dissolution of cement particles caused by adsorbed SP molecules. Irrespective of the mechanism, the precipitation of C-S-H and the consequent formation of the rigid network proposed by Roussel et al. [60] are delayed in the presence of SP. In turn, viscosity is the macroscopic signature of the flow of water in the porosity of the granular system [64], so it depends primarily on the particle concentration of the suspension [65]. Ettringite precipitation consumes a great amount of water (chemical formula $Ca_6Al_2(SO_4)_3(OH)_{12}\cdot 26H_2O$) and starts in the very first minutes of hydration, even in the presence of SP. Jansen et al. [66] and Pott et al. [67] observed ettringite contents of 4-7 wt% in cement pastes with SP already at 10 minutes of hydration through *in-situ* XRD. This relation between the ettringite content and the viscosity of cement paste was confirmed by Jakob et al. [68] by coupling time-resolved rheological tests and *in-situ* XRD. These reports explain why the yield stress of the pastes with SP did not significantly change within the first 60 minutes, but the viscosity did.

When comparing the different sonication conditions, although SP sonication apparently increased the viscosity of paste at the first measurement (mentioned earlier), the viscosity increase over time was higher for the paste with non-sonicated SP than for those containing sonicated SP. In fact, significant differences (higher than the testing variability) can be observed from 90 min onward. In this regard, Kirby and Lewis [69] and Winnefeld et al. [47] evaluated the effect of the molecular architecture of different SPs on the rheology and hydration of cement pastes. The authors found that SPs with reduced chain length and molecular weight lead to higher delays in cement hydration. This would result in a slower formation of hydrated products (e.g., C-S-H and ettringite) responsible for the yield stress and viscosity increases over time discussed earlier. Thus, although SP sonication reduced its initial dispersing ability, sonication improved the time-dependent dispersing performance of the admixture. These results are in line with those from Peng et al. [55], which observed that SPs with high molecular weight had greater initial dispersing capacity but lower dispersion stabilization over time, i.e., dispersion ability after 60 minutes.

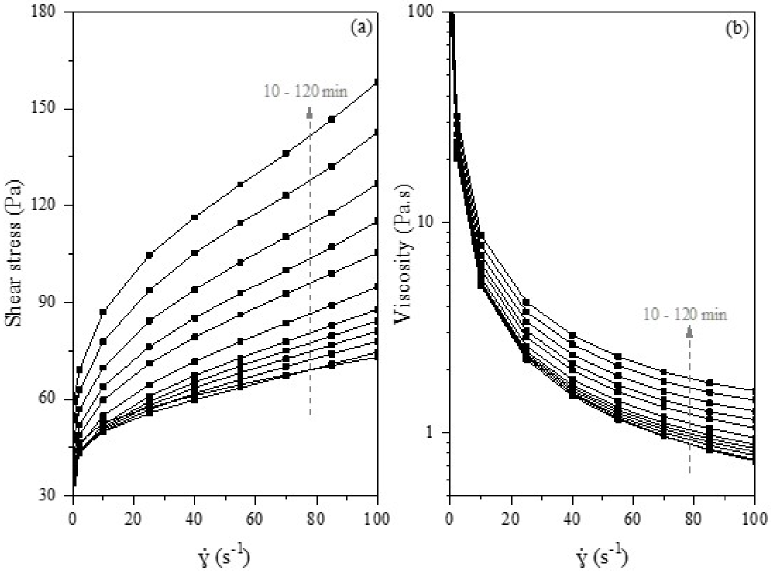

Figure 8. Example of flow curves (a) and viscosity vs. shear rate curves (b) of SP cement paste during the first 120 min of hydration.

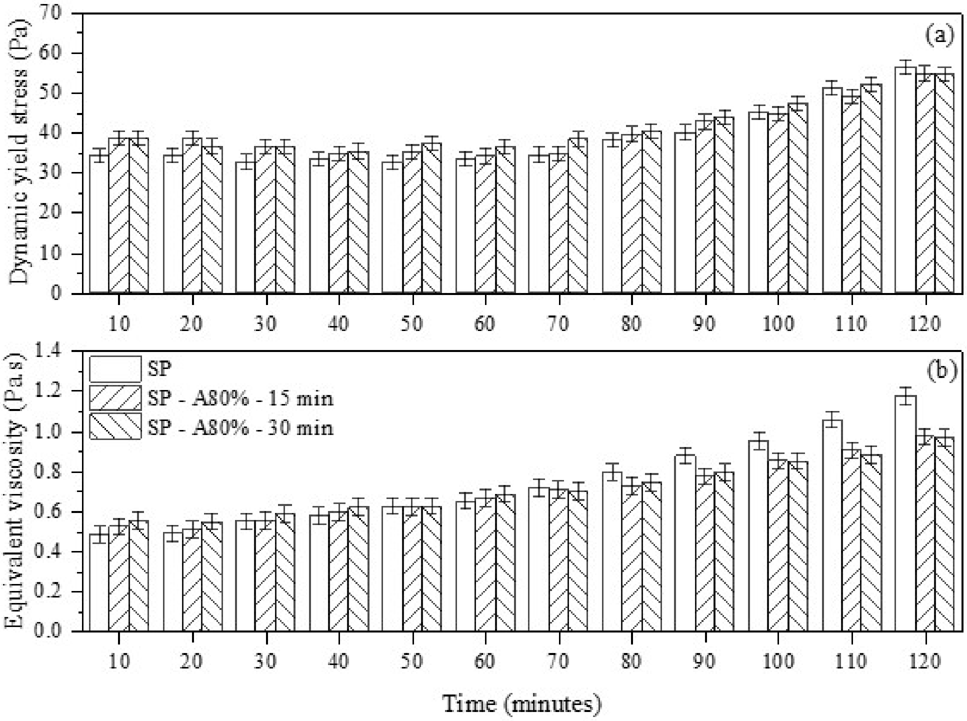

Figure 9. Dynamic yield stress (a) and equivalent viscosity (b) of the pastes over time.

3.3. Compressive strength

Figure 10 shows the compressive strength of the pastes at 14 and 28 days of hydration. Overall, the cement pastes evaluated showed compressive strength values around 65 MPa and 75 MPa at 14 and 28 days, respectively. Although the SP sonication affected the fresh properties of the cement pastes, it did not affect the compressive strength at the ages evaluated. ANOVA (summarized in Table 4) indicated that the amplitude and duration of sonication do not exert a significant influence on the compressive strength of paste. Moreover, no statistical differences were observed between the strength values of the cement pastes evaluated according to the Tukey test conducted.

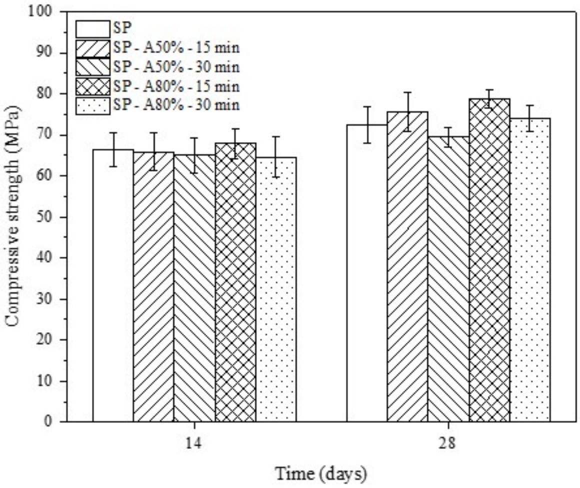

Figure 10. Compressive strength of the pastes.

Table 4. Two-way ANOVA of compressive strength results.

Factor	Sum of squares (SS)	Degrees of freedom (DF)	Mean square (MS)	P value	
Amplitude (A)	100.335	2	50.167	0.247	Not significant
Duration (B)	69.423	2	34.711	0.373	Not significant
A x B	98.068	4	24.517	0.582	Not significant
Error	776.245	23	33.749	-	-

4 CONCLUSIONS

This work assessed the effect of sonicating polycarboxylate-based SP used in cementitious composites. DLS and zeta potential results suggested that sonication reduced the length of SP chains. In cement pastes, sonication reduced the initial dispersion capacity of SP, resulting in samples with increased yield stress, viscosity, and hysteresis area values at the first measurement (10 minutes) compared to those from paste produced with non-sonicated SP. In contrast, SP sonication improved the particle dispersion improving the maintenance of dispersion over time, observed by the lower increases in viscosity for the sonicated SP samples up to 120 minutes. Finally, SP sonication did not significantly affect the compressive strength of the pastes at 14 and 28 days. Therefore, when SP is sonicated together with nanoparticles for application in cementitious matrices, the effect of sonicating the chemical admixture must be considered when the fresh-state properties of the composite are evaluated.

ACKNOWLEDGEMENTS

The governmental agencies CAPES, CNPq, FAPESC from Brazil provided financial support for the study. The Interdisciplinary Laboratory for the Development of Nanostructures (LINDEN – UFSC) is acknowledged for carrying out the DLS analysis. XRD analyses were conducted in the Laboratory of X-ray Diffraction (LDRX – UFSC) multiuser facility.

REFERENCES

[1] L. Silvestro et al., "Influence of ultrasonication of functionalized carbon nanotubes on the rheology, hydration, and compressive strength of portland cement pastes," *Materials*, vol. 14, no. 18, pp. 5248, Sep 2021, http://dx.doi.org/10.3390/ma14185248.

[2] M. S. Konsta-Gdoutos, P. A. Danoglidis, M. G. Falara, and S. F. Nitodas, "Fresh and mechanical properties, and strain sensing of nanomodified cement mortars: The effects of MWCNT aspect ratio, density and functionalization," *Cement Concr. Compos.*, vol. 82, pp. 137–151, 2017, http://dx.doi.org/10.1016/j.cemconcomp.2017.05.004.

[3] P. A. Danoglidis, M. S. Konsta-Gdoutos, and S. P. Shah, "Relationship between the carbon nanotube dispersion state, electrochemical impedance and capacitance and mechanical properties of percolative nanoreinforced OPC mortars," *Carbon N. Y.*, vol. 145, pp. 218–228, 2019, http://dx.doi.org/10.1016/j.carbon.2018.12.088.

[4] L. Silvestro, A. Spat Ruviaro, P. Ricardo de Matos, F. Pelisser, D. Zambelli Mezalira, and P. Jean Paul Gleize, "Functionalization of multi-walled carbon nanotubes with 3-aminopropyltriethoxysilane for application in cementitious matrix," *Constr. Build. Mater.*, vol. 311, pp. 125358, 2021, http://dx.doi.org/10.1016/j.conbuildmat.2021.125358.

[5] L. Silvestro, G. T. D. S. Lima, A. S. Ruviaro, and P. J. P. Gleize, "Stability of carboxyl-functionalized carbon nanotubes in simulated cement pore solution and its effect on the compressive strength and porosity of cement-based nanocomposites," *C - J Carbon Res*, vol. 8, no. 3, pp. 39, Jul 2022, http://dx.doi.org/10.3390/c8030039.

[6] Y. Sargam and K. Wang, "Influence of dispersants and dispersion on properties of nanosilica modified cement-based materials," *Cement Concr. Compos.*, vol. 118, pp. 103969, 2021, http://dx.doi.org/10.1016/j.cemconcomp.2021.103969.

[7] X. Liu, P. Hou, and H. Chen, "Effects of nanosilica on the hydration and hardening properties of slag cement," *Constr. Build. Mater.*, vol. 282, pp. 122705, 2021, http://dx.doi.org/10.1016/j.conbuildmat.2021.122705.

[8] Y. S. B. Fraga, J. H. S. Rêgo, V. M. S. Capuzzo, D. S. Andrade, and P. C. Morais, "Ultrasonication and synergistic effects of silica fume and colloidal nanosilica on the C–S–H microstructure," *J. Build. Eng.*, vol. 32, pp. 101702, 2020, http://dx.doi.org/10.1016/j.jobe.2020.101702.

[9] L. U. D. Tambara Jr. et al., "Effect of the nanosilica source on the rheology and early-age hydration of calcium sulfoaluminate cement pastes," *Constr. Build. Mater.*, vol. 327, pp. 126942, 2022, http://dx.doi.org/10.1016/j.conbuildmat.2022.126942.

[10] G. T. S. Lima, A. Zaleski, L. U. D. Tambara Jr., J. C. Rocha, F. Pelisser, and P. J. P. Gleize, "Evaluation of the effect of nanosilica and recycled fine aggregate in Portland cement rendering mortars," *Rev. IBRACON Estrut. Mater.*, vol. 15, no. 5, e15509, 2022, http://dx.doi.org/10.1590/s1983-41952022000500009.

[11] N. H. Azevedo, P. R. Matos, P. J. P. Gleize, and A. M. Betioli, "Effect of thermal treatment of SiC nanowhiskers on rheological, hydration, mechanical and microstructure properties of Portland cement pastes," *Cement Concr. Compos.*, vol. 117, pp. 103903, 2021., http://dx.doi.org/10.1016/j.cemconcomp.2020.103903.

[12] N. H. Azevedo and P. J. P. Gleize, "Effect of silicon carbide nanowhiskers on hydration and mechanical properties of a Portland cement paste," *Constr. Build. Mater.*, vol. 169, pp. 388–395, Apr 2018, http://dx.doi.org/10.1016/j.conbuildmat.2018.02.185.

[13] Y. Lan et al., "Preliminary investigation on silicon carbide whisker-modified cement-based composites," *Open Ceram.*, vol. 6, pp. 100107, 2021, http://dx.doi.org/10.1016/j.oceram.2021.100107.

[14] N. Hamed, M. S. El-Feky, M. Kohail, and E. S. A. R. Nasr, "Effect of nano-clay de-agglomeration on mechanical properties of concrete," *Constr. Build. Mater.*, vol. 205, pp. 245–256, 2019, http://dx.doi.org/10.1016/j.conbuildmat.2019.02.018.

[15] M. A. Mirgozar Langaroudi and Y. Mohammadi, "Effect of nano-clay on workability, mechanical, and durability properties of self-consolidating concrete containing mineral admixtures," *Constr. Build. Mater.*, vol. 191, pp. 619–634, 2018, http://dx.doi.org/10.1016/j.conbuildmat.2018.10.044.

[16] E. D. Rodríguez, S. A. Bernal, J. L. Provis, J. Payá, J. M. Monzó, and M. V. Borrachero, "Structure of Portland cement pastes blended with sonicated silica fume," *J. Mater. Civ. Eng.*, vol. 24, no. 10, pp. 1295–1304, 2012, http://dx.doi.org/10.1061/(ASCE)MT.1943-5533.0000502.

[17] K. M. Liew, M. F. Kai, and L. W. Zhang, "Carbon nanotube reinforced cementitious composites: an overview," *Compos., Part A Appl. Sci. Manuf.*, vol. 91, pp. 301–323, 2016, http://dx.doi.org/10.1016/j.compositesa.2016.10.020.

[18] T. Selvamani, S. Anandan, A. M. Asiri, P. Maruthamuthu, and M. Ashokkumar, "Preparation of $MgTi_2O_5$ nanoparticles for sonophotocatalytic degradation of triphenylmethane dyes," *Ultrason. Sonochem.*, vol. 75, pp. 105585, 2021, http://dx.doi.org/10.1016/j.ultsonch.2021.105585.

[19] T. Manzur and N. Yazdani, "Strength enhancement of cement mortar with carbon nanotubes: early results and potential," *Transp. Res. Rec.*, vol. 2142, no. 1, pp. 102–108, 2010, http://dx.doi.org/10.3141/2142-15.

[20] L. Assi et al., "Multiwall carbon nanotubes (MWCNTs) dispersion & mechanical effects in OPC mortar & paste: a review," *J. Build. Eng.*, vol. 43, pp. 102512, 2021, http://dx.doi.org/10.1016/j.jobe.2021.102512.

[21] L. Silvestro and P. Jean Paul Gleize, "Effect of carbon nanotubes on compressive, flexural and tensile strengths of Portland cement-based materials: a systematic literature review," *Constr. Build. Mater.*, vol. 264, pp. 120237, Dec 2020, http://dx.doi.org/10.1016/j.conbuildmat.2020.120237.

[22] M. Liebscher et al., "Impact of the molecular architecture of polycarboxylate superplasticizers on the dispersion of multi-walled carbon nanotubes in aqueous phase," *J. Mater. Sci.*, vol. 52, no. 4, pp. 2296–2307, 2017, http://dx.doi.org/10.1007/s10853-016-0522-3.

[23] B. S. Sindu and S. Sasmal, "Properties of carbon nanotube reinforced cement composite synthesized using different types of surfactants," *Constr. Build. Mater.*, vol. 155, pp. 389–399, 2017, http://dx.doi.org/10.1016/j.conbuildmat.2017.08.059.

[24] S. Ma, Y. Qian, and S. Kawashima, "Performance-based study on the rheological and hardened properties of blended cement mortars incorporating palygorskite clays and carbon nanotubes," *Constr. Build. Mater.*, vol. 171, pp. 663–671, 2018, http://dx.doi.org/10.1016/j.conbuildmat.2018.03.121.

[25] M. O. Mohsen, N. Al-Nuaimi, R. K. Abu Al-Rub, A. Senouci, and K. A. Bani-Hani, "Effect of mixing duration on flexural strength of multi walled carbon nanotubes cementitious composites," *Constr. Build. Mater.*, vol. 126, pp. 586–598, 2016, http://dx.doi.org/10.1016/j.conbuildmat.2016.09.073.

[26] A. Sedaghatdoost and K. Behfarnia, "Mechanical properties of Portland cement mortar containing multi-walled carbon nanotubes at elevated temperatures," *Constr. Build. Mater.*, vol. 176, pp. 482–489, 2018, http://dx.doi.org/10.1016/j.conbuildmat.2018.05.095.

[27] T. Jarolim, M. Labaj, R. Hela, and K. Michnova, "Carbon Nanotubes in Cementitious Composites: Dispersion, Implementation, and Influence on Mechanical Characteristics," *Adv. Mater. Sci. Eng.*, vol. 2016, pp. 1–6, 2016, http://dx.doi.org/10.1155/2016/7508904.

[28] P. C. Ma, N. A. Siddiqui, G. Marom, and J. K. Kim, "Dispersion and functionalization of carbon nanotubes for polymer-based nanocomposites: A review," *Compos., Part A Appl. Sci. Manuf.*, vol. 41, no. 10, pp. 1345–1367, 2010, http://dx.doi.org/10.1016/j.compositesa.2010.07.003.

[29] J. E. L. Siqueira and P. J. P. Gleize, "Effect of carbon nanotubes sonication on mechanical properties of cement pastes," *Rev. IBRACON Estrut. Mater.*, vol. 13, no. 2, pp. 455–463, 2020, http://dx.doi.org/10.1590/s1983-41952020000200013.

[30] M. H. Dehghani, A. Zarei, and M. Yousefi, "Efficiency of ultrasound for degradation of an anionic surfactant from water: Surfactant determination using methylene blue active substances method," *MethodsX*, vol. 6, pp. 805–814, 2019, http://dx.doi.org/10.1016/j.mex.2019.03.028.

[31] T. Campbell and M. R. Hoffmann, "Sonochemical degradation of perfluorinated surfactants: Power and multiple frequency effects," *Separ. Purif. Tech.*, vol. 156, pp. 1019–1027, 2015, http://dx.doi.org/10.1016/j.seppur.2015.09.053.

[32] P. S. Bhandari, B. P. Makwana, and P. R. Gogate, "Microwave and ultrasound assisted dual oxidant based degradation of sodium dodecyl sulfate: Efficacy of irradiation approaches and oxidants," *J. Water Process Eng.*, vol. 36, pp. 101316, 2020, http://dx.doi.org/10.1016/j.jwpe.2020.101316.

[33] T. Poinot, K. Benyahia, A. Govin, T. Jeanmaire, and P. Grosseau, "Use of ultrasonic degradation to study the molecular weight influence of polymeric admixtures for mortars," *Constr. Build. Mater.*, vol. 47, pp. 1046–1052, 2013, http://dx.doi.org/10.1016/j.conbuildmat.2013.06.007.

[34] M.-N. Noirfontaine, M. Courtial, F. Dunstetter, G. Gasecki, and M. Signes-Frehel, "Tricalcium silicate Ca_3SiO_5 superstructure analysis: a route towards the structure of the M_1 polymorph," *Z. Kristallogr.*, vol. 227, no. 2, pp. 102–112, 2012, http://dx.doi.org/10.1524/zkri.2012.1425.

[35] M. Palacios and F. Puertas, "Stability of superplasticizer and shrinkage-reducing admixtures in high basic media," *Mater. Constr.*, vol. 8, no. 4, pp. 683–691, 2018.

[36] S. Li, J. Zhang, Z. Li, Y. Gao, and C. Liu, "Feasibility study of red mud-blast furnace slag based geopolymeric grouting material : Effect of superplasticizers," *Constr. Build. Mater.*, vol. 267, pp. 120910, 2021, http://dx.doi.org/10.1016/j.conbuildmat.2020.120910.

[37] Y. Alrefaei, Y. S. Wang, and J. G. Dai, "The effectiveness of different superplasticizers in ambient cured one-part alkali activated pastes," *Cement Concr. Compos.*, vol. 97, pp. 166–174, 2019, http://dx.doi.org/10.1016/j.cemconcomp.2018.12.027.

[38] E. Janowska-Renkas, "The effect of superplasticizers' chemical structure on their efficiency in cement pastes," *Constr. Build. Mater.*, vol. 38, pp. 1204–1210, 2013, http://dx.doi.org/10.1016/j.conbuildmat.2012.09.032.

[39] H. Bessaies-Bey, R. Baumann, M. Schmitz, M. Radler, and N. Roussel, "Effect of polyacrylamide on rheology of fresh cement pastes," *Cement Concr. Res.*, vol. 76, pp. 98–106, 2015, http://dx.doi.org/10.1016/j.cemconres.2015.05.012.

[40] H. Bessaies-Bey, R. Baumann, M. Schmitz, M. Radler, and N. Roussel, "Organic admixtures and cement particles: Competitive adsorption and its macroscopic rheological consequences," *Cement Concr. Res.*, vol. 80, pp. 1–9, Feb 2016, http://dx.doi.org/10.1016/j.cemconres.2015.10.010.

[41] X. Wang, Y. Yang, X. Shu, Y. Wang, Q. Ran, and J. Liu, "Tailoring polycarboxylate architecture to improve the rheological properties of cement paste," *J. Dispers. Sci. Technol.*, vol. 40, no. 11, pp. 1567–1574, 2019, http://dx.doi.org/10.1080/01932691.2018.1485578.

[42] F. De Larrard, C. F. Ferraris, and T. Sedran, "Fresh concrete: a Herschel-Bulkley material," *Mater. Struct. Constr.*, vol. 31, no. 211, pp. 494–498, 1996, http://dx.doi.org/10.1007/bf02480474.

[43] P. A. Wedding and D. L. Kantro, "Influence of water-reducing admixtures on properties of cement paste: a miniature slump test," *Cem. Concr. Aggreg.*, vol. 2, no. 2, pp. 95, 1980, http://dx.doi.org/10.1520/CCA10190J.

[44] American Society for Testing and Materials, *Standard Practice for Use of Unbonded Caps in Determination of Compressive Strength of Hardened Cylindrical Concrete Specimens*, ASTM C1231/C1231M, 2015.

[45] P. Alafogianni, K. Dassios, S. Farmaki, S. K. Antiohos, T. E. Matikas, and N. M. Barkoula, "On the efficiency of UV-vis spectroscopy in assessing the dispersion quality in sonicated aqueous suspensions of carbon nanotubes," *Colloids Surf. A Physicochem. Eng. Asp.*, vol. 495, pp. 118–124, 2016, http://dx.doi.org/10.1016/j.colsurfa.2016.01.053.

[46] Y. Ma, J. Bai, C. Shi, S. Sha, and B. Zhou, "Effect of PCEs with different structures on hydration and properties of cementitious materials with low water-to-binder ratio," *Cement Concr. Res.*, vol. 142, pp. 106343, 2021, http://dx.doi.org/10.1016/j.cemconres.2020.106343.

[47] F. Winnefeld, S. Becker, J. Pakusch, and T. Götz, "Effects of the molecular architecture of comb-shaped superplasticizers on their performance in cementitious systems," *Cement Concr. Compos.*, vol. 29, no. 4, pp. 251–262, 2007, http://dx.doi.org/10.1016/j.cemconcomp.2006.12.006.

[48] M. Ezzat, X. Xu, K. El Cheikh, K. Lesage, R. Hoogenboom, and G. De Schutter, "Structure-property relationships for polycarboxylate ether superplasticizers by means of RAFT polymerization," *J. Colloid Interface Sci.*, vol. 553, pp. 788–797, 2019, http://dx.doi.org/10.1016/j.jcis.2019.06.088.

[49] X. Qiu, X. Peng, C. Yi, and Y. Deng, "Effect of side chains and sulfonic groups on the performance of polycarboxylate-type superplasticizers in concentrated cement suspensions," *J. Dispers. Sci. Technol.*, vol. 32, no. 2, pp. 203–212, 2011, http://dx.doi.org/10.1080/01932691003656888.

[50] N. Roussel, *Understanding the Rheology of Concrete.* Cambridge: Woodhead Publishing, 2011. http://dx.doi.org/10.1533/9780857095282.

[51] H. Feng, Z. Feng, W. Wang, Z. Deng, and B. Zheng, "Impact of polycarboxylate superplasticizers (PCEs) with novel molecular structures on fluidity, rheological behavior and adsorption properties of cement mortar," *Constr. Build. Mater.*, vol. 292, pp. 123285, 2021, http://dx.doi.org/10.1016/j.conbuildmat.2021.123285.

[52] S. L. Malhotra, "“Ultrasonic degradation of hydroxypropyl cellulose solutions in water, ethanol, and tetrahydrofuran," *J. Macromol. Sci. Part A Chem.*, vol. 17, no. 4, pp. 601–636, 1982, http://dx.doi.org/10.1080/00222338208062411.

[53] S. G. Erzengin, K. Kaya, S. Perçin Özkorucuklu, V. Özdemir, and G. Yıldırım, "The properties of cement systems superplasticized with methacrylic ester-based polycarboxylates," *Constr. Build. Mater.*, vol. 166, pp. 96–109, 2018, http://dx.doi.org/10.1016/j.conbuildmat.2018.01.088.

[54] R. Magarotto, I. Torresan, and N. Zeminian, “Influence of the molecular weight of polycarboxylate ether superplasticizers on the rheological properties of fresh cement pastes, mortar and concrete,” in *Proc. 11th Int. Congr. Chem. Cem.*, 2003, pp. 514–526.

[55] X. Peng, C. Yi, X. Qiu, and Y. Deng, "Effect of molecular weight of polycarboxylate-type superplasticizer on the rheological properties of cement pastes," *Polym. Polymer Compos.*, vol. 20, no. 8, pp. 725–736, 2012, http://dx.doi.org/10.1177/096739111202000808.

[56] M. Palacios, F. Puertas, P. Bowen, and Y. F. Houst, "Effect of PCs superplasticizers on the rheological properties and hydration process of slag-blended cement pastes," *J. Mater. Sci.*, vol. 44, no. 10, pp. 2714–2723, 2009, http://dx.doi.org/10.1007/s10853-009-3356-4.

[57] L. N. Assi, Y. A. J. Al-Hamadani, E. E. Deaver, V. Soltangharaei, P. Ziehl, and Y. Yoon, "Effect of sonicated deionized water on the early age behavior of portland cement-based concrete and paste," *Constr. Build. Mater.*, vol. 247, pp. 118571, 2020, http://dx.doi.org/10.1016/j.conbuildmat.2020.118571.

[58] S. Ziembowicz, M. Kida, and P. Koszelnik, "The impact of selected parameters on the formation of hydrogen peroxide by sonochemical process," *Separ. Purif. Tech.*, vol. 204, pp. 149–153, 2018, http://dx.doi.org/10.1016/j.seppur.2018.04.073.

[59] Y. Liu, Z. Zhang, R. Jing, and P. Yan, "The interaction of sodium citrate and polycarboxylate-based superplasticizer on the rheological properties and viscoelasticity of cement-based materials," *Constr. Build. Mater.*, vol. 293, pp. 123466, 2021, http://dx.doi.org/10.1016/j.conbuildmat.2021.123466.

[60] N. Roussel, G. Ovarlez, S. Garrault, and C. Brumaud, "The origins of thixotropy of fresh cement pastes," *Cement Concr. Res.*, vol. 42, no. 1, pp. 148–157, 2012, http://dx.doi.org/10.1016/j.cemconres.2011.09.004.

[61] M. Y. A. Mollah, W. J. Adams, R. Schennach, and D. L. Cocke, "Review of cement-superplasticizer interactions and their models," *Adv. Cement Res.*, vol. 12, no. 4, pp. 153–161, 2000, http://dx.doi.org/10.1680/adcr.2000.12.4.153.

[62] F. Ridi, L. Dei, E. Fratini, S. H. Chen, and P. Baglioni, "Hydration kinetics of tri-calcium silicate in the presence of superplasticizers," *J. Phys. Chem. B*, vol. 107, no. 4, pp. 1056–1061, 2003, http://dx.doi.org/10.1021/jp027346b.

[63] J. Rieger, J. Thieme, and C. Schmidt, "Study of precipitation reactions by X-ray microscopy: $CaCO_3$ precipitation and the effect of polycarboxylates," *Langmuir*, vol. 16, no. 22, pp. 8300–8305, 2000, http://dx.doi.org/10.1021/la0004193.

[64] F. De Larrard and T. Sedran, "Mixture-proportioning of high-performance concrete," *Cement Concr. Res.*, vol. 32, no. 11, pp. 1699–1704, 2002., http://dx.doi.org/10.1016/S0008-8846(02)00861-X.

[65] I. M. Krieger and T. J. Dougherty, "A mechanism for non-newtonian flow in suspensions of rigid spheres," *Trans. Soc. Rheol.*, vol. 3, no. 1, pp. 137–152, 1959, http://dx.doi.org/10.1122/1.548848.

[66] D. Jansen, J. Neubauer, F. Goetz-Neunhoeffer, R. Haerzschel, and W.-D. Hergeth, "Change in reaction kinetics of a Portland cement caused by a superplasticizer: calculation of heat flow curves from XRD data," *Cement Concr. Res.*, vol. 42, no. 2, pp. 327–332, Feb 2012, http://dx.doi.org/10.1016/j.cemconres.2011.10.005.

[67] U. Pott, C. Jakob, D. Jansen, J. Neubauer, and D. Stephan, "Investigation of the incompatibilities of cement and superplasticizers and their influence on the rheological behavior," *Materials*, vol. 13, no. 4, pp. 977, 2020, http://dx.doi.org/10.3390/ma13040977.

[68] C. Jakob et al., "Relating ettringite formation and rheological changes during the initial cement hydration: a comparative study applying XRD analysis, rheological measurements and modeling," *Materials*, vol. 12, no. 18, pp. 2957, 2019, http://dx.doi.org/10.3390/ma12182957.

[69] G. H. Kirby and J. A. Lewis, "Comb polymer architecture effects on the rheological property evolution of concentrated cement suspensions," *J. Am. Ceram. Soc.*, vol. 87, no. 9, pp. 1643–1652, Sep 2004, http://dx.doi.org/10.1111/j.1551-2916.2004.01643.x.

Author contributions: LS: Conceptualization, formal analysis, data curation; LS, GL, AR: methodology; LS, AR: investigation; PRM, ER, PG: resources; LS, GL, AR: writing—original draft preparation; LS, PRM, PG: writing—review and editing; PG: supervision; PRM, ER, PG: funding acquisition.

Editors: Bernardo Tutikian, Guilherme Aris Parsekian.